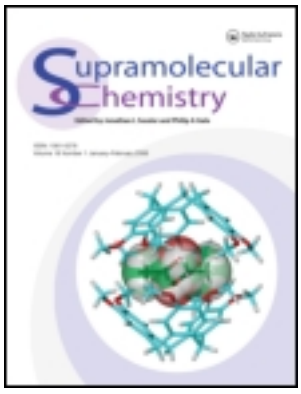

Supramolecular Chemistry
Publication details, including instructions for authors and subscription information:
http://www.tandfonline.com/loi/gsch20

Enantioselective recognition of electrochemically inactive phenylalanine by thiolated-cyclodextrin/ferrocene-coated gold nanoparticles

Yinghui Bian [a], Guifen Zhang [a], Xian Zhong [a], Demei Tian [a] & Haibing Li [a]
[a] Key Laboratory of Pesticide & Chemical Biology (CCNU), Ministry of Education, College of Chemistry, Central China Normal University, Wuhan, 430079, P.R. China

Available online: 15 Apr 2011

To cite this article: Yinghui Bian, Guifen Zhang, Xian Zhong, Demei Tian & Haibing Li (2011): Enantioselective recognition of electrochemically inactive phenylalanine by thiolated-cyclodextrin/ferrocene-coated gold nanoparticles, Supramolecular Chemistry, 23:6, 455-461

To link to this article: http://dx.doi.org/10.1080/10610278.2010.544738

Supramolecular Chemistry
Vol. 23, No. 6, June 2011, 455–461

Taylor & Francis
Taylor & Francis Group

Enantioselective recognition of electrochemically inactive phenylalanine by thiolated-cyclodextrin/ferrocene-coated gold nanoparticles

Yinghui Bian, Guifen Zhang, Xian Zhong, Demei Tian and Haibing Li*

Key Laboratory of Pesticide & Chemical Biology (CCNU), Ministry of Education, College of Chemistry, Central China Normal University, Wuhan 430079, P.R. China

(*Received 5 October 2010; final version received 6 November 2010*)

An electrochemical sensor for enantioselective recognition of electrochemically inactive phenylalanine (Phe) with high sensitivity was reported in this paper. The sensor was fabricated by the approach of thiolated β-cyclodextrin (SH-CD) assembled with Au nanoparticles, which were deposited on the glassy carbon electrode surface. The modified electrode was characterised by atomic force microscopy, X-ray photoelectron spectroscopy, attenuated total reflection IR spectroscopy, scanning electron microscopy and contact angle. The sensor was used to conduct the enantioselective recognition of chiral Phe, and offered detection limits as low as 84 nM (S/N = 3). The possible mechanism underlying was discussed.

Keywords: electrochemical sensor; enantioselective recognition; β-cyclodextrin; Au nanoparticles; glassy carbon electrode

1. Introduction

It is well known that analysis of chiral molecules is a very useful tool in biological, pharmaceutical, clinical, foods or environmental fields (*1*). In this sense, chiral analysis of amino acids is thus a remarkably important methodology for providing a better understanding of life science, nutrition, safety, microbiology, metabolic pathways, etc. of the organisms in which these molecules are found (*2–8*). Up to now, gas chromatography (*9*), liquid chromatography (*10*), GC/MS (*11*) and capillary electrophoresis (*12*) have all been used for analysing chiral amino acids. However, for efficient separation and sensitive detection, these techniques exhibit some drawbacks, such as the use of expensive chiral columns, laborious sample pretreatments, complicated derivatising procedures and relatively lengthy analysis time (*13–15*). Therefore, the convenient, time saving and reliable method is generally required for the chiral detection of amino acids (*16*). Electrochemical sensor is a simple and inexpensive, yet and highly sensitive analytical technique with real-time output. In this sense, the use of electrochemical sensors for enantiomeric recognition of amino acids has generated interest in the field (*17*).

For the construction of chiral interface, self-assembled monolayers (SAMs) are often used for introducing chiral host molecule onto the surface of electrode. For example, Levon and co-workers (*18*) have reported a chiral sensor based on the ITO plate modified with chiral *N*-carbobenzoxy-aspartic acids (N-CBZ-Asp) *via* surface imprinting technology. However, the extensive application of chiral sensors based on the SAMs is restricted, because of low sensitivity. More recently, much attention has been paid to the development of interfacing supramolecular chemistry and nanotechnology with the ability of molecular recognition (*19–22*). Recent research in this field has focused on the synthetic acceptors based on the host molecule such as crown ether, calixarene or cyclodextrin (CD)-functionalised metal nanoparticles with unique properties as compared to small molecules, including the binding site tuning, high sensitivity, low cost. Particularly, due to their large specific surface Au nanoparticles (Au NPs), modified electrodes are utilised to enhance the amount of host molecule immobilised onto the electrode leading to an improvement of the sensor performance. Moreover, the use of Au NPs in this kind of analytical systems contributes to facilitate the electron transfer between the redox indicator and the electrode surface by acting as tiny conduction centres (*23*). A methyl parathion electrochemical sensor constructed by *para*-Sulphonatocalix[6]arene-modified silver nanoparticles has been developed by our group; the detection limit (DL) is 4.0 nM (S/N = 3) (*24*). Nowadays, the interest on surface-bound CDs has increased significantly. CDs are cyclic oligosaccharides consisting of six to eight D-(+)-glucopyranose units, providing chiral recognition of various organic molecules (*25*, *26*). Peng et al. (*27*) fabricated one ascorbic acid electrochemical sensor on the basis of β-CD-modified ITO electrode with the DL of 4.1 μM. However, to our knowledge, there has been no report on chiral surfaces

*Corresponding author. Email: lhbing@mail.ccnu.edu.cn

ISSN 1061-0278 print/ISSN 1029-0478 online

DOI: 10.1080/10610278.2010.544738
http://www.informaworld.com

combined with CDs functionalised Au NPs for electrochemical enantioselective recognition of amino acids.

In this paper, we described an electrochemical sensor for enantioselectivity of electrochemically inactive phenylalanine (Phe) on the basis of thiolated β-cyclodextrin (SH-CD) and Au NPs. The electrochemical sensor was constructed by depositing Au NPs on glassy carbon electrode surface (Au NPs/GCE) firstly, and then the complexes of SH-CD/ferrocene (Fc) were assembled on the surface of Au NPs/GCE. The sensor exhibited recognition properties towards L-Phe, which could displace the Fc adsorbed in the CD cavity. The DL of L-Phe was 84 nM (S/N = 3). The sensor opens new opportunities for enantioselective recognition.

2. Experimental section

2.1 Chemicals and materials

All chemicals used were of analytical grade reagents. Reagent grade β-CD, Fc and amino acids were purchased from Sigma-Aldrich (St Louis, MO, USA). The primary alcohol groups on the lower rim of β-CD were thiolated according to the procedure reported previously (*28*). Double-distilled water was used for all experiments.

2.2 The construction of electrochemical sensor

A GCE was polished to a mirror finish with 0.3 and 0.05 μm of alumina slurry and then washed ultrasonically in nitric acid (v:v = 1:1), absolute ethanol and water for 3 min, respectively, and dried at room temperature. A 0.1 M KNO_3 aqueous solution containing 0.1 mM $HAuCl_4$ was used for electrodeposition of Au NPs at GCE electrodes. For electrodeposition, a fixed potential of −0.30 V was applied at the GCE electrodes for 60 s. Then, the electrode was dipped into stirred water for 10 min to wash the $AuCl_4^-$ adsorbed on the surface. The modified electrode Au NPs/GCE was obtained.

The film was constructed via dipping the Au NPs/GCE in a solution prepared by mixing corresponding SH-CD water and Fc ethanol solutions to make up final concentrations of 0.60 mM SH-CD and 0.60 mM Fc for 12 h. The SH-CD SAMs were formed on the Au NPs/GCE surface. The obtained film was denoted as Fc/SH-CD/Au NPs on the surface of GCE.

2.3 Electrochemical and surface wetting property measurements

The conventional three-electrode system with platinum wire was used as auxiliary electrode, saturated calomel electrode as reference and Fc/CD/Au NPs/GCE as working electrode. The KNO_3 solution (0.1 M) containing Fc (0.30 mM) was used as the supporting electrolyte (v_{H_2O}/v_{Et_2O} = 1:1). The modified electrode was immersed into the electrolyte, and cyclic voltammetry was performed on the modified electrode, which was recorded between −0.40 and +0.70 V. The wetting property was measured by static contact angle measurements, which were performed with a water droplet (10 ± 1 μl) using an OCA 20 contact angle system (DataPhysics Instruments, Filderstadt, Germany) at 25°C.

2.4 Equipment

Electrochemical measurements were performed on CHI-660C workstation (Shanghai Chen Hua Instruments, Shanghai, China) with a conventional three electrode. Atomic force microscopy (AFM) images were obtained by using the Dimension 3100 (Veeco Instruments, Inc., Santa Barbara, CA, USA) in the tapping mode. X-ray photoelectron spectroscopic (XPS) images were gained by PHI Quantera SXM. Scanning electron microscopy (SEM) was recorded by a Hitachi S-4700 electron microscope. The static water contact angle was measured at 25°C by means of an OCA 20 contact angle system (DataPhysics Instruments). Attenuated total reflection Fourier-transform infrared spectrum (ATR-FTIR) was acquired with a Nexus 470 FTIR (Thermo Nicolet Corporation, Nicolet, USA).

3. Results and discussion

3.1 Characterisation of the SH-CD/Au NPs/GCE

Au NPs were electrochemically deposited onto the GCE surface by applying a potential value of −0.3 V for 60 s. Then, SH-CD and Fc assembled with Au NPs/GCE, as shown in Scheme 1. The XPS spectra of Fc/SH-CD/Au NPs and SH-CD/Au NPs on bare GCE, as shown in Figure S1 (available online), demonstrated that Fc and SH-CDs were successfully modified onto gold nanoparticles. As shown in Figure S1A (available online), 163.99 eV peak was assigned to S2p peak, which suggests that SH-CDs are attached successfully. Fe 2p peak (709.15 eV), as shown in Figure S1B (available online), is attributed to Fc adsorbed onto the surface. As shown in the SEM images of Au NPs/GCE and SH-CD/Au NPs/GCE in Figure 1, it was obviously observed that the Au NPs were deposited on the surface of the GCE. As shown in the SEM images, Au NPs

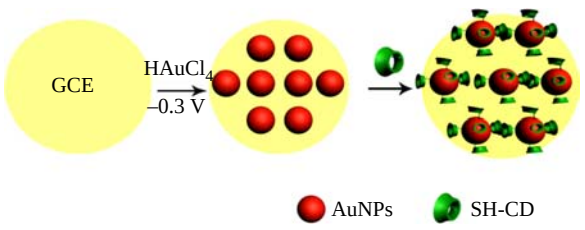

Scheme 1. Schematic diagram for the deposition of Au NPs on the surface of the GCE and assembling SH-CD and Fc.

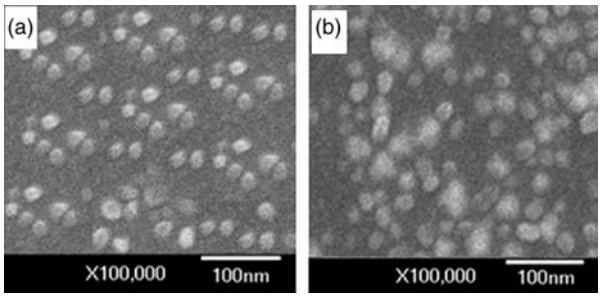

Figure 1. SEM images of (a) Au NPs/GCE and (b) SH-CD/Au NPs/GCE, the bars are 100 nm.

were monodisperse and uniform. The sizes of Au NPs increased after the surface modification (Figure 1(b)). The surface morphology and the size distribution of Au NPs and SH-CD/Au NPs were characterised by AFM images in Figure 2, respectively. The average size of bare and modified gold nanoparticles was 9.5 and 12 nm, respectively. It indicated that a layer of SH-CD was assembled on the surface of gold nanoparticles due to the length of a β-CD molecule measuring 1.2 nm (*29*). When FT-IR spectra of SH-CD were compared with those of SH-CD/Au NPs as shown in Figure S2 (available online), prominent S–H vibrational band at 2577 cm^{-1} (Figure S2a, available online) disappeared in IR spectrum of SH-CD/Au NPs GCE (Figure S2b, available online). These results conformed the successful bonding of the SH-CD onto the surface of Au nanoparticles via a thiolate linkage (*30–33*).

3.2 Impedance characterisation of the SH-CD/Au NPs/GCE

The voltammetric behaviour of a 5-mM ferricyanide was studied. Figure 3(A) shows (a) cyclic voltammograms (CVs) of bare GCE, (b) Au NPs/GCE and (c) SH-CD/Au NPs/GCE, respectively, in 5 mM $[Fe(CN)_6]^{4-/3-}$/0.1 M KNO_3 at 100 mV/s over the range of −0.4 to +0.6 V. For the bare GCE, an electrochemical response for $[Fe(CN)_6]^{4-/3-}$ with peak potential separation of 246 mV was observed (scan a). Au NPs-modified electrode induced higher current intensity (scan b), which implied that Au NPs provided an excellent conductive interface to improve electron transfer between the ferricyanide and the electrode surface. When SH-CD was modified on the Au NPs/GCE, current intensity decreased (scan c). These results indicate that the presence of the organic molecules blocks the electron transfer between the ferricyanide and the electrode surface, which was the indirect evidence of SH-CD bonding with Au NPs covalently.

By using the $Fe(CN)_6^{4-/3-}$ redox couple as the electrochemical probe, the Nyquist plots of different electrodes in the frequency range from 0.01 to 100,000 Hz were obtained (Figure 3(B)). The redox process of the probe showed electron-transfer resistance of about 280 Ω (curve a), 150 Ω (curve b) and 340 Ω (curve c) at bare GCE, Au NPs/GCE and CD/Au NPs/GCE, respectively. The results were corresponding to the voltammetric behaviour of electrodes, which suggested that the modified electrode SH-CD/Au/GCE was successfully fabricated. Compared to

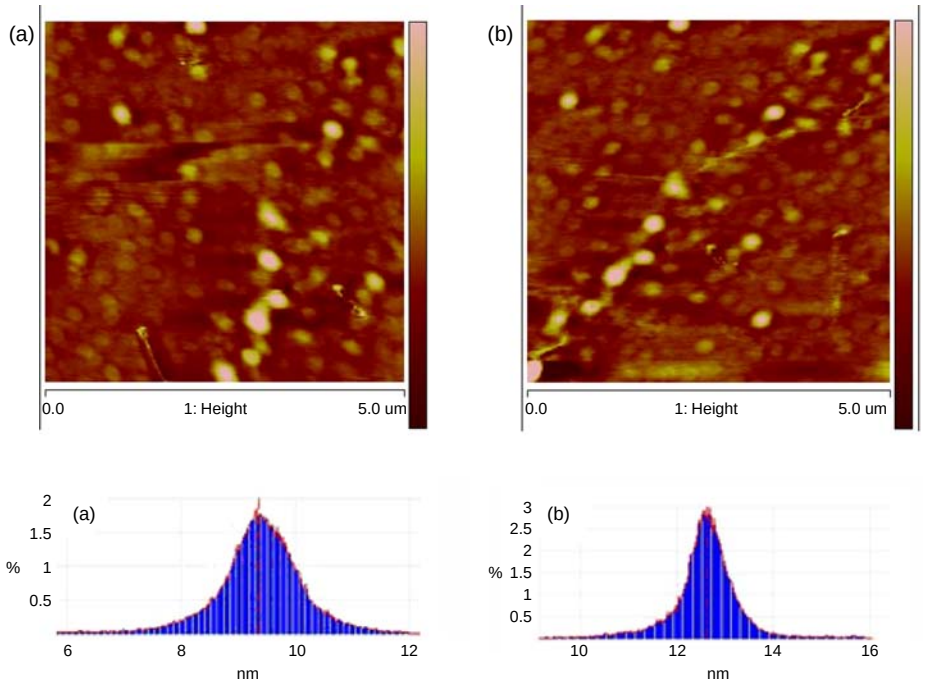

Figure 2. AFM images and the particle analysis showing the Au NPs deposited on GCE (a) and SH-CD assembled on the Au NPs on the surface of GCE (b).

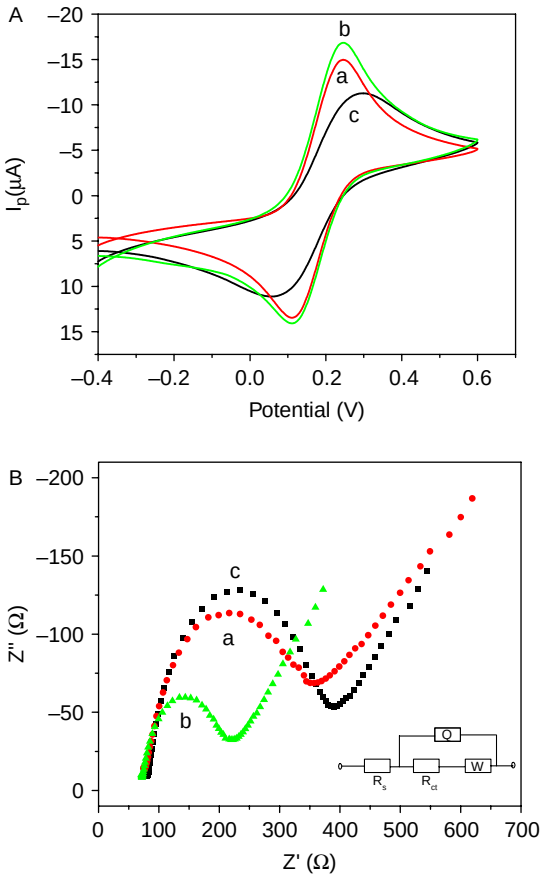

Figure 3. CVs and electrochemical impedance spectroscopy of (a) bare GCE; (b) Au NPs/GCE; (c) SH-CD/Au NPs/GCE in the electrolyte containing 5.0 mM $Fe(CN)_6^{3-/4-}$ and 0.1 M KNO_3 at the scan rate of 100 mV s^{-1}.

Au/GCE, there are more SH-CD binding sites on the electrode surface, which allowed SH-CD/Au/GCE to detect much lower concentrations of solutes (as low as 10^{-7} M) than that of bare Au/GCE (Figure S3, available online).

A linear correlation exists between the logarithm of I_p recorded for 0.3 mM Fc in the solution and the logarithm of the scan rate (ν) over the range of 0.1 to 10 V s^{-1}, as shown in Figure S4 (available online). The linear equation is $R = 1.184 + 1.1860 \times \log(\nu)$ with a linearity coefficient of 0.999, indicating that the electrochemical oxidation of Fc at the SH-CD-modified electrode displays the surface-controlled processes (*34*). It suggests that CD on the surface can bind Fc.

3.3 *Enantioselective analysis of Phe*

When the Fc/SH-CD/Au NPs/GCE was exposed to the solution containing 3×10^{-4} M Fc and 10^{-3} M L-Phe, the anodic current of Fc reduced distinctly, while no obvious change of Fc oxidation current was found in the solution containing 3×10^{-4} M Fc and 10^{-3} M D-Phe (Figure 4). Such a large difference in the oxidation current change makes this sensor practically useful for the enantioselective recognition of the chiral L-Phe.

To further prove the selectivity of L-Phe, control experiments were carried out. As shown in Figure 5, when the Fc/SH-CD/Au NPs/GCE was exposed to the solutions containing other L/D-amino acids, viz, Alanine, Valine, Methionine, Proline, Tryptophan, Threonine, Cysteine, Tyrosine, Aspartic acid, Glutamic acid, Lysine, Arginine and Histidine, respectively. A rare change was found for the oxidation current of Fc. This phenomenon indicates that the modified electrode Fc/SH-CD/Au NPs/GCE has excellent selectivity to L-Phe. The specific selectivity of L-Phe is due to the favoured binding of L-Phe by the SH-CD (*34*). L-Phe prefers binding with SH-CD to form more stable supramolecular complexes, which inhibited the electron transfer from Fc to electrode surface (*35*).

To further prove the mechanism of enantioselective recognition of L-Phe, the bonding constants of SH-CD, Fc and L-Phe were measured by an electrochemical technique (*36*, *37*). The formation constant K_f for the Fc/SH-CD

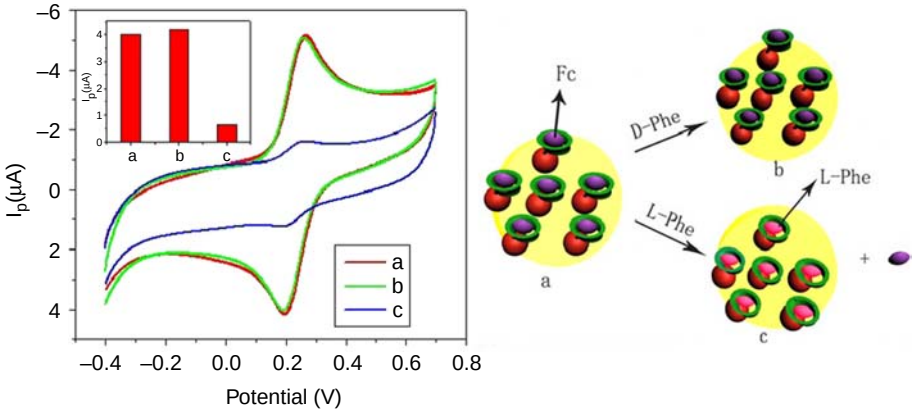

Figure 4. CVs of SH-CD/Au NPs/GCE in the electrolyte containing 0.10 M KNO_3 and (a) 0.30 mM Fc; (b) 0.30 mM Fc + 1 mM D-Phe; (c) 0.30 mM Fc + 1 mM L-Phe; scan rate, 100 mV s^{-1}.

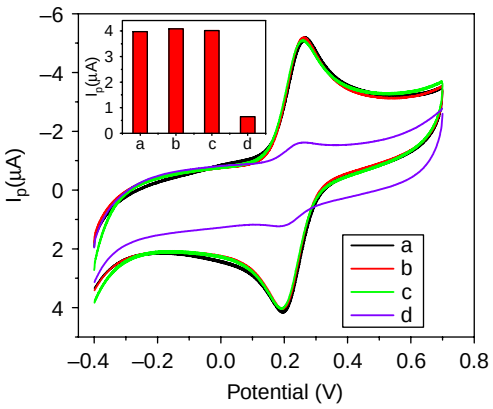

Figure 5. CVs of SH-CD/Au NPs/GCE in the electrolyte containing 0.10 M KNO_3 and (control) 0.30 mM Fc; (a) 0.30 mM Fc + 1 mM L-amino acids; (b) 0.30 mM Fc + 1 mM D-amino acids; (c) 0.30 mM Fc + 1 mM D-Phe; (d) 0.30 mM Fc + 1 mM L-Phe.

inclusion complex was obtained from the plot employing the equation

$$\frac{[\mathrm{Fc}]}{I_\mathrm{p}} = \frac{1}{K_\mathrm{f} C} + \frac{[\mathrm{Fc}]}{C}, \tag{1}$$

which has been derived based on the Langmuir isotherm (*35*, *36*).

Here, I_p is the CV peak current at a guest concentration (Fc), C is a constant and K_f is the formation constant. The SH-CD adsorbed onto the electrode surface acts as the host molecule here, while Fc in solution acts as the electroactive guest molecule.

When an electrochemically inert molecule L-Phe forms a stronger complex with the SH-CD, it will replace the electroactive Fc, lowering the oxidation or reduction current of Fc. The difference in current, ΔI, observed in the presence and absence of the electrochemically inert molecule is related to its formation constant with the host molecule on the surface via the following equation (*34*, *36*, *37*)

$$\frac{[\text{L-Phe}]}{\Delta I} = A\left\{\frac{K_\mathrm{f}[\mathrm{Fc}]+1}{K_{\text{L-Phe,f}}} + [\text{L-Phe}]\right\}, \tag{2}$$

where

$$A = \frac{1 + K_\mathrm{f}[\mathrm{Fc}]}{c[\text{SH-CD}]_0}. \tag{3}$$

Here, $K_{\text{L-Phe,f}}$ is the formation constant of the SH-CD with L-Phe, $[\text{SH-CD}]_0$ is the concentration of the SH-CD on the SH-CD/Au NPs/GCE surface, which is constant under the experimental conditions used here and c is the current per mole of Fc molecule. From Equation (1), the formation constant K_f can be obtained from the plot of $[\mathrm{Fc}]/I_\mathrm{p}$ versus [Fc], and similarly, the formation constant of SH-CD with L-Phe $K_{\text{L-Phe,f}}$ can be determined from Equation (2) by appropriately plotting the experimental data.

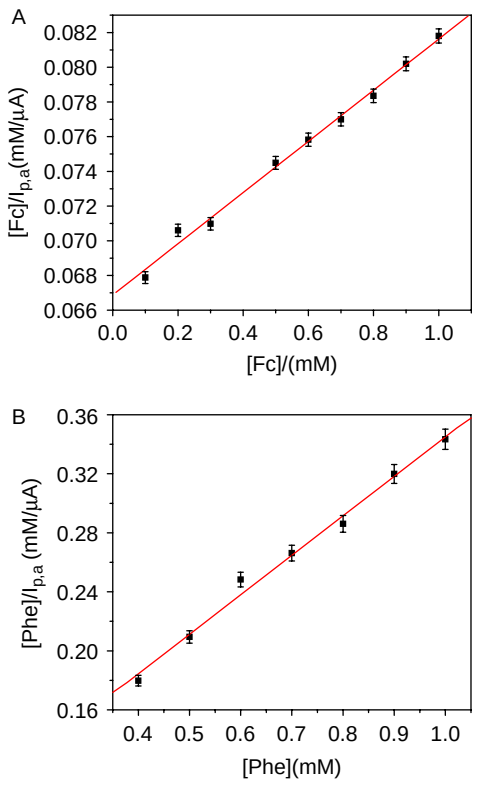

Figure 6. (A) $[\mathrm{Fc}]/I_{\mathrm{p,a}}$ versus [Fc] plot, the currents used here were obtained in water–ethanol (v:v = 1:1) solutions containing 0.10 M KNO_3 and various Fc concentrations (B) $[\mathrm{Phe}]/I_{\mathrm{p,a}}$ versus [Phe] plot, the currents used here were obtained in water–ethanol solutions (v:v = 1:1) containing 0.30 mM Fc, 0.10 M KNO_3 and various L-Phe concentrations. The scan rates were 100 mV s^{-1}.

Figure 6(A) shows a $[\mathrm{Fc}]/I_\mathrm{p}$ versus [Fc] plot for the Fc-SH-CD complex according to Equation (1). It can be seen from Figure 6(A) that the values of $[\mathrm{Fc}]/I_\mathrm{p}$ increased linearly with increasing Fc concentrations from 0.10 to 1.0 mM. A formation constant between the SH-CD and Fc complex is calculated to be 220.5 M^{-1}. Similarly, from the plot according to Equation (2) (Figure 6(B)), the formation constants of L-Phe with immobilised SH-CD are calculated to be 3691.6 M^{-1} in water–ethanol (v:v = 1:1) solution containing 0.30 mM Fc and 0.10 M KNO_3. It is obvious that L-Phe forms a significantly stronger complex with SH-CD than Fc does; thus, L-Phe in solution could replace Fc captured in the SH-CD cavities, leading to the anodic current of Fc reduced distinctly.

3.4 The wetting property of the modified electrode measured

The wetting property of the electrodes surface after pretreatment was characterised by the contact angles measurement of the electrodes. Figure 7 shows the images

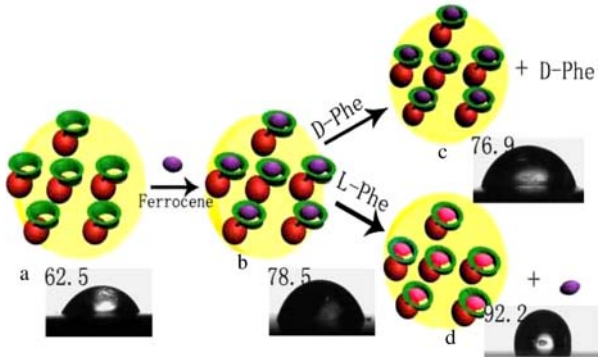

Figure 7. Schematic diagram of Fc/SH-CD/Au/GCE for L-Phe recognition and the photos of contact angle measurements using a water droplet on the surface of (a) SH-CD/Au/GCE, (b) Fc/SH-CD/Au/GCE, (c) Fc/SH-CD/Au/GCE (after being dipped in D-Phe), (d) Fc/SH-CD/Au/GCE (after being dipped in L-Phe).

of a drop of water on the electrodes surface. The contact angles of (a) SH-CD/Au/GCE and (b) Fc/SH-CD/Au/GCE are 62° and 78.5°, respectively. The contact angle of the Fc/SH-CD/Au NPs/GCE (92.2°) dipped in the solution containing L-Phe is bigger than that of the Fc/SH-CD/Au/GCE. This phenomenon demonstrates that the L-Phe takes the place of Fc, leading to the wetting property of the Fc/SH-CD/Au NPs/GCE surface change simultaneously. When the Fc/SH-CD/Au/GCE is dipped in the solution containing D-Phe(c), the contact angle (76.9°) is found to be similar to that of Fc/SH-CD/Au/GCE, which indicated that the D-Phe could not take the place of the Fc, and the wetting property of the modified electrode surface barely changed.

3.5 *Analytical performance*

Figure 8 shows a series of CVs recorded in the presence of various amounts of L-Phe with the concentration of Fc kept constant at 0.30 mM in water–ethanol (v:v = 1:1) solution containing 0.10 M KNO_3. The CV currents decreased when the concentration of L-Phe increased in solution. A linear relationship ($R = 0.984$) between the current and the L-Phe concentration was obtained in the range of 0.1–1 μM. The linear regression equation is ΔI_p (μA) $= -4.41 + 627.7C$. The DL of the sensor was 84 nM (S/N = 3), which was lower than the reported value of 5.0 μM of N-CBZ-Asp (*18*). It has been reported that Fc and SH-CD are easy to form host–guest complex (*38–40*), β-CD can form host–guest complex with L-Phe more easily than D-Phe and can be used for chiral distinction (*41–43*). The formation constant of host–guest complex between Fc and SH-CD is 220.5 M^{-1}, while the formation constant between SH-CD and L-Phe is 3691.6 M^{-1}, which

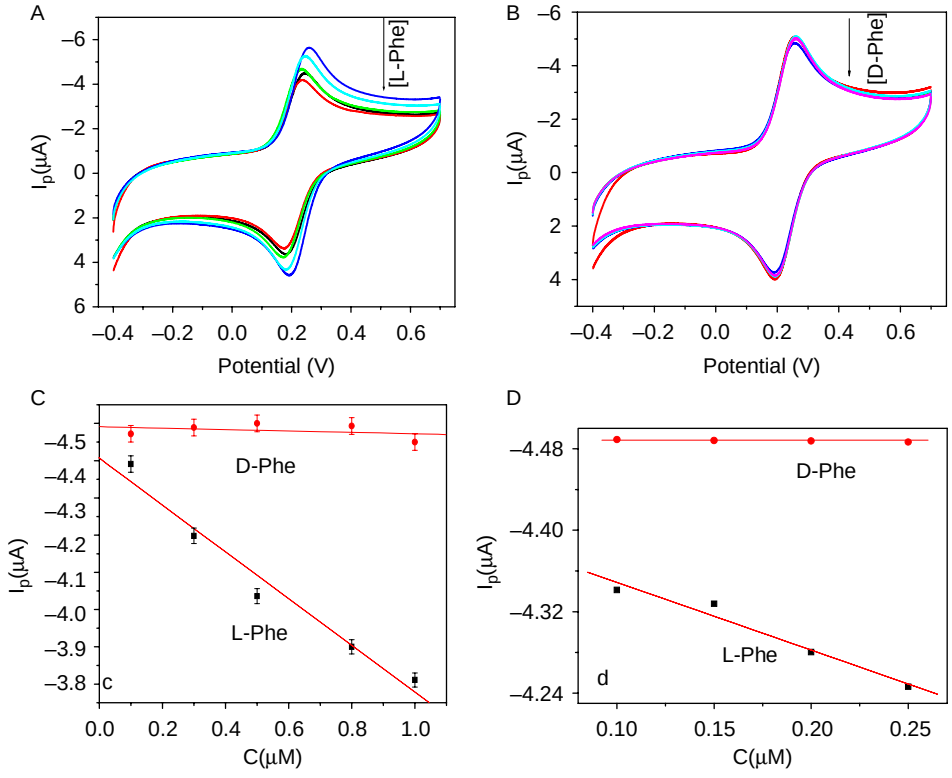

Figure 8. CVs of Fc/SH-CD/AuNPs/GCE in the electrolyte of water and ethanol (v:v = 1:1) containing 0.10 M KNO_3 and 0.30 mM Fc and 0.10, 0.30, 0.50, 0.80, 1.0 μM Phe (a,b) and the connection between the largest current intensity and the concentration of Phe (c). And the small concentration of Phe ranging from 0.1 to 0.25 μM (d).

is calculated by the experiment. When the substrates of D/L-Phe are added to the solution, we can find different changes of Fc redox current: L-Phe can decrease the current intensity, while D-Phe cannot affect the current change of Fc. As shown in the experiment, the intensity of the current gradually reduced as L-Phe was added, but not D-Phe. According to the result of the experiment, it is implied that the SH-CD/Au NPs-modified GCE surface is capable of effectively detecting L-Phe by means of the SH-CD as receptor sites.

4. Conclusion

In summary, we have demonstrated in this work that a new electrochemical sensor on the basis of SH-CD/Au NPs acts as an enantioselective sensing platform to electrochemically inactive L-Phe. Compared to the SAMs-modified electrode, SH-CD/AuNPs/GCE could sensitively detect L-Phe. The L-Phe molecules fit well to the cavity of SH-CD and compete with the Fc, forming an insertion complex, which induced electrochemical signal and the wetting property of the sensor surface changes. Studies are in progress to construct the electrochemical sensor on the basis of this complete mechanism to detect other electrochemically inactive compounds and to achieve the enantioselective recognition of chiral compounds.

Acknowledgements

This work was financially supported by the National Natural Science Foundation of China (20772038), 863 program (2009AA06A417), Program for Excellent Research Group of Hubei Province (2009CDA048) and self-determined research funds of CCNU from the colleges' basic research and operation of MOE (CCNU09AO200).

References

(1) Armstrong, D.W.; Chang, C.D.; Li, W.L. *J. Agric. Food Chem.* **1990**, *38*, 1674–1677.
(2) Friedman, M. *J. Agric. Food Chem.* **1999**, *47*, 3457–3479.
(3) Simo, C.; Barbas, C.; Cifuentes, A. *Electrophoresis* **2003**, *24*, 2431–2441.
(4) Simo, C.; Barbas, C.; Cifuentes, A. *J. Agric. Food Chem.* **2002**, *50*, 5288–5293.
(5) Simo, C.; Alvarez, P.J.M.; Barbas, C.; Cifuentes, A. *Electrophoresis* **2004**, *25*, 2885–2891.
(6) Bednar, P.; Aturki, Z.; Stransky, Z.; Fanali, S. *Electrophoresis* **2001**, *22*, 2129–2135.
(7) Helfman, P.M.; Bada, J.L.; Zigler, J.L. *Nature* **1977**, *268*, 71–73.
(8) Mann, E.H.; Sandhouse, M.E.; Burg, J.; Fisher, G.H. *Science* **1983**, *220*, 1407–1408.
(9) Zumwalt, R.W., Kuo, K.C., Gehrke, C.W., Eds.; *Amino Acid Analysis by Gas Chromatography*; CRC Press: Boca Raton, FL, 1987; Vols. I, III.
(10) Deyl, Z.; Hyanek, J.; Horikova, M. *J. Chromatogr.* **1986**, *379*, 177–250.
(11) Duncan, M.W.; Poljak, A. *Anal. Chem.* **1998**, *70*, 890–896.
(12) Prata, C.; Bonnafous, P.; Fraysse, N.; Treilhou, M.; Poinsot, V.; Couderc, F. *Electrophoresis* **2001**, *22*, 4129–4138.
(13) Yokoyama, T.; Tanaka, Y.; Sato, M.; Kan-No, N.; Nakano, T.; Yamaguchi, T.; Nagahisa, E. *Fish. Sci.* **2005**, *71*, 924–930.
(14) Erbe, T.; Brückner, H. *Eur. Food Res. Technol.* **2000**, *211*, 6–12.
(15) Erbe, T.; Bruckner, H.; Lebensm, Z. *Unters. Forsch. A* **1998**, *207*, 400–409.
(16) Schultz, C.L.; Moini, M. *Anal. Chem.* **2003**, *75*, 1508–1513.
(17) Privett, B.J.; Shin, J.H.; Schoenfisch, M.H. *Anal. Chem.* **2008**, *80*, 4499–4517.
(18) Zhou, Y.X.; Yu, B.; Levon, K. *Chem. Mater.* **2003**, *15*, 2774–2779.
(19) Nishiyabu, R.; Hashimoto, N.; Cho, T.; Watanabe, K.; Yasunaga, T.; Endo, A.; Kaneko, K.; Niidome, T.; Murata, M.; Adachi, C.; Katayama, Y.; Hashizume, M.; Kimizuka, N. *J. Am. Chem. Soc.* **2009**, *131*, 2151–2158.
(20) Park, I.K.; Recum, A.; Jiang, S.Y.; Pun, S.H. *Langmuir* **2006**, *22*, 8478–8484.
(21) Forrest, M.L.; Gabrielson, N.; Pack, D.W. *Biotechnol. Bioeng.* **2004**, *89*, 416–423.
(22) Pun, S.H.; Davis, M. *Bioconj. Chem.* **2002**, *13*, 630–639.
(23) Bharathi, S.; Nogami, M.; Ikeda, S. *Langmuir* **2001**, *17*, 1–4.
(24) Bian, Y.H.; Li, C.Y.; Li, H.B. *Talanta* **2010**, *81*, 1028–1033.
(25) Xiao, Y.C.; Lim, H.M.; Chung, T.S.; Rajagopalan, R. *Langmuir* **2007**, *23*, 12990–12996.
(26) Schneiderman, E.; Stalcup, A.M. *J. Chromatogr B* **2000**, *745*, 83–102.
(27) Zuo, F.; Luo, C.H.; Zheng, Z.H.; Ding, X.B.; Peng, Y.X. *Electroanalysis* **2008**, *20*, 894–899.
(28) Diao, G.W.; Qian, C.; Chen, M.; Huang, Y. *J. Supramol. Chem.* **2006**, *18*, 117.
(29) Dong, Z.Y.; Liu, J.Q.; Mao, S.Z. *J. Am. Chem. Soc.* **2004**, *126*, 16395–16404.
(30) Templeton, A.C.; Chen, S.; Gross, S.M.; Murray, R.W. *Langmuir* **1999**, *15*, 66–76.
(31) Xiong, D.J.; Chen, M.L.; Li, H.B. *Chem. Commun.* **2008**, 880–882.
(32) Han, C.P.; Zeng, L.L.; Li, H.B.; Xie, G.Y. *Sens. Actuators B* **2009**, *137*, 704–709.
(33) Yao, Y.; Tian, D.M.; Li, H.B. *ACS Appl. Mater. Interf.* **2010**, *2*, 684–690.
(34) Choi, S.J.; Choi, B.G.; Park, S.M. *Anal. Chem.* **2002**, *74*, 1998–2002.
(35) Freeman, R.; Finder, T.; Bahshi, L.; Willner, I. *Nano Lett.* **2009**, *9*, 2073–2076.
(36) Kitano, H.; Taira, Y.; Yamamoto, H. *Anal. Chem.* **2000**, *72*, 2976–2980.
(37) Maeda, Y.; Fukuda, T.; Yamamoto, H.; Kitano, H. *Langmuir* **1997**, *13*, 4187–4189.
(38) Frasconi, M.; Andrea, D.A.; Gabriele, F. *Langmuir* **2009**, *25*, 12937–12944.
(39) Domi, Y.; Yoshinaga, Y.; Shimazu, K. *Langmuir* **2009**, *25*, 8094–8100.
(40) Han, Y.B.; Cheng, K.; Simon, A.K. *J. Am. Chem. Soc.* **2006**, *128*, 13913–13920.
(41) Freeman, R.; Finder, T.l.; Bahshi, L.L. *Nano Lett.* **2009**, *9*, 2073–2076.
(42) Han, C.P.; Li, H.B. *Small* **2008**, *4*, 1344–1350.
(43) Xiao, Y.C.; Lim, H.M.; Chung, T.S. *Langmuir* **2007**, *23*, 12990–12996.